Electrochemical and Spectral Analysis of the Long-Range Interactions between the Q_o and Q_i Sites and the Heme Prosthetic Groups in Ubiquinol–Cytochrome *c* Oxidoreductase†

Neil Howell*

Department of Radiation Therapy, Department of Human Biological Chemistry & Genetics, The University of Texas Medical Branch, Galveston, Texas 77550

Dan E. Robertson

Johnson Research Foundation, Department of Biochemistry and Biophysics, University of Pennsylvania, Philadelphia, Pennsylvania 19104

Received October 26, 1992; Revised Manuscript Received July 1, 1993®

ABSTRACT: The results are presented of an electrochemical and high-resolution spectral analysis of the heme prosthetic groups in the bc_1 complex from mouse cells. To study the long-range interactions between the Q_o and Q_i quinone redox sites and the b heme groups, we analyzed the effects on the proximal and distal *b* heme groups, and the c_1 heme, of inhibitors that tightly and specifically bind to the Q_i or Q_o redox site. A number of results emerged from these studies. (1) There is inhomogeneous broadening of the *b* heme α band absorption spectra. Futhermore, contrary to the conclusion from low-resolution spectral analysis, the higher energy transition in the split-α band spectrum of the b_L heme is more intense than the lower energy transition. (2) Inhibitors that bind at the Q_i site have significant effects upon the electronic environment of the distal b_L heme. Conversely, Q_o site inhibitors induced changes in the electronic environment of the distal b_H heme. (3) In contrast, inhibitor binding at either site has little effect upon the midpoint potential of the distal heme. (4) Experiments in which *both* a Q_i and a Q_o inhibitor are bound at the redox sites indicate that the long-range effects of one inhibitor are not blocked by the second inhibitor; enhanced effects are often observed. (5) In the double-inhibitor titrations involving the Q_o inhibitor myxothiazol, there is evidence for two electrochemically and spectrally distinct species of the b_L heme group, a phenomenon not observed previously. (6) The high-resolution deconvolutions of α band absorption spectra allow an interpretation of these inhibitor-induced changes in terms of homogeneous broadening, inhomogeneous broadening, and changes in x–y degeneracy. The general conclusion from these experiments is that when an inhibitor binds to a quinone redox site of the cytochrome *b* protein, it produces local conformational changes that, in turn, are transmitted to distal regions of the protein. The ligation of the b_H and b_L hemes between two parallel transmembrane helices provides a mechanism by which long-distance interactions can be propagated. The lack of long-range effects upon the midpoint potentials of the heme groups suggests, however, that protein conformational changes are unlikely to be a major control mechanism for the transmembrane electron- and proton-transfer steps of the Q cycle.

Mammalian cytochrome bc_1 complexes (complex III; ubiquinol–cytochrome *c* oxidoreductase) contain 11 protein subunits, three of which carry redox prosthetic groups (Schagger et al., 1986). In addition to a high-potential Fe-S[1] center, the complexes contain cytochrome c_1 and the bis-heme cytochrome *b*. The prokaryotic bc_1 complexes are structurally simpler with three of four protein subunits but the same redox prosthetic groups (Trumpower, 1990). There is now general agreement that the transfer of reducing equivalents from ubiquinol to cytochrome *c* catalyzed by the bc_1 complex occurs through the Q cycle mechanism that was first proposed by Mitchell (1976) and subsequently refined by other investigators (Bowyer & Trumpower, 1981; Rich, 1984; Crofts, 1985; West, 1989; Ding et al., 1992). The Q cycle (Figure 1) postulates that within the bc_1 complex there are *two* redox catalytic sites, a ubiquinol oxidizing site at the proton output side of the membrane (designated here as Q_o) and a ubiquinone reducing site on the proton input side of the membrane (Q_i).[2] The complete Q cycle involves the oxidation of two quinol molecules at the Q_o site and the reduction of one quinone at the Q_i site with the *net* oxidation of one quinol and the reduction of two cytochrome *c* molecules.

The presence of two quinone redox sites in bc_1 complexes has been strongly supported by the characterization of inhibitors that specifically block either the Q_o site (Myxothiazol, mucidin, stigmatellin) or the Q_i site [antimycin A, funiculosin; reviewed in von Jagow and Link (1986)]. Analysis of the electrogenic steps of the Q cycle indicates that the Q_o site and the b_L heme group are at one side of the membrane with the b_H heme approximately midway through the mem-

† This research was supported by Research Grants GM33683 (N.H.) and GM27309 (P. L. Dutton) from the National Institutes of Health.

* Author to whom correspondence should be addressed at Biology Division F56, Department of Radiation Therapy, The University of Texas Medical Branch, Galveston, TX 77550.

® Abstract published in *Advance ACS Abstracts,* September 15, 1993.

[1] Abbreviations: FeS, Rieske iron–sulfur protein; E_m, midpoint potential *versus* standard hydrogen electrode; E_h, ambient redox potential *versus* standard hydrogen electrode; SMP, submitochondrial particles; HOMO, highest occupied molecular orbital; LUMO, lowest unoccupied molecular orbital.

[2] This center has been designated Q_p or Q_Z in previous publications on the mitochondrial and photosynthetic bacterial complexes, respectively, while the Q_i center has been denoted as Q_n or Q_c.

0006-2960/93/0432-11162$04.00/0

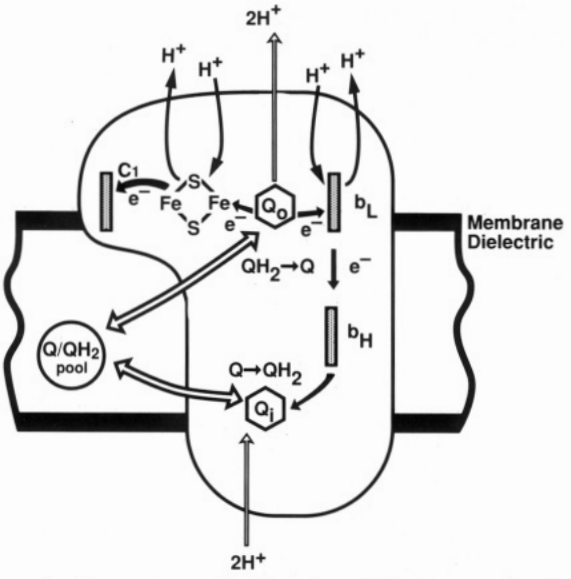

FIGURE 1: The proton-motive Q cycle and the topography of the heme prosthetic groups and redox sites within the membrane dielectric. The heme groups are denoted by stippled bars. Electron transfers are shown by heavy solid arrows. As a result of the fact that two quinol molecules are oxidized at the Q_o site and that one quinone molecule is reduced at the Q_i site, for each complete turn of the Q cycle, there is a net transmembrane movement of two protons from the proton input side of the membrane to the proton output side (narrow open arrows); for further details, see Ding et al. (1992).

brane low dielectric and the Q_i site at the opposite side of the membrane (Robertson & Dutton, 1988). Through a combination of secondary structural modeling (Crofts et al., 1987; Brasseur, 1988), analysis of evolutionarily conserved regions (Hauska et al., 1988; Howell, 1989), determination of which cytochrome *b* residues are altered in inhibitor-resistant mutants (di Rago & Colson, 1988; Howell & Gilbert, 1988; Daldal et al., 1989; di Rago et al., 1989), site-directed mutagenesis of highly conserved residues (Atta-Asafo-Adjei & Daldal, 1991; Yun et al., 1991, 1992; Hacker et al., 1993), and biophysical studies (Robertson & Dutton, 1988; Ohnishi et al., 1989; Robertson et al., 1990), a consensus is emerging of the regions of the cytochrome *b* protein that contribute structurally to the Q_o and Q_i sites [e.g., Figure 6 of Howell (1989)].

The present state of knowledge, therefore, encompasses a good understanding of the basic redox chemistry of Q cycle catalysis[3] and some crude, but improving, ideas on the functional topography of the cytochrome *b* protein (Figure 1). The bc_1 complex, however, is probably not a rigid matrix of redox prosthetic groups, and there may be long-range interactions among the FeS centers, the heme groups, and the Q_i and Q_o redox centers. Thus, the E_m value of the b_H heme group is coupled to the redox status of the quinone molecule bound to the Q_i site (Salerno et al., 1989; Rich et al., 1990). Second, circular dichroic studies suggest that the cytochrome *b* heme groups may be excitonically coupled (Degli Esposti et al., 1989). Third, inhibitors that bind at one site within the bc_1 complex may have long-range effects. In the bc_1 complex from yeast, the Q_i site inhibitor funiculosin raises the E_m values of both the b_H heme group and the FeS center (Tsai & Palmer, 1982). In addition, there are isolated reports that Q_i and Q_o inhibitors alter the spectrum of the distal heme group [e.g., Rich et al. (1990)]. The involvement of long-range interactions in the control of electron and/or proton transfer during the Q cycle, however, has not been rigorously or systematically investigated. To gain further insights into the interactions among the Q_o and Q_i redox catalytic sites and the heme prosthetic groups, a comprehensive electrochemical and high-resolution spectral analysis has been undertaken of the long-range effects upon the heme prosthetic groups of the bc_1 complex of inhibitors that bind at the Q_o and Q_i quinone redox sites.

[3] It should be noted that while the Q cycle has the status of biochemical orthodoxy, there remains some controversy over the operation of the Q cycle in chloroplast b_6f complexes (Furbacher et al., 1990), and there are unresolved issues such as the precise nature of the electrogenic events and the topography of the Q_i and Q_o sites within the membrane dielectric [*e.g.*, Konstantinov (1990) and Beattie et al. (1992)].

MATERIALS AND METHODS

Partial Purification of the bc_1 Complex. The LA9TK mouse fibroblast cell line was used for the experiments reported here. Cells were cultured and crude mitochondria were isolated after digitonin cell permeabilization as described previously (Howell & Nalty, 1987). Suspensions of the final mitochondrial pellet were adjusted to 50% glycerol and stored at −80 °C.

Partial purification of the bc_1 complex was carried out using the procedure of Ljungdahl et al. (1986) with the modifications to be described. All steps were carried out at 0–4 °C. Approximately 3000–3500 mg of crude mitochondria were thawed and pooled, diluted with an approximately equal volume of buffer containing 50 mM Tris-HCl and 1 mM $MgCl_2$ (pH 8.0 at 4°), and pelleted by centrifugation at 15 000 rpm (an SS-34 Sorvall rotor was used throughout) for 15 min. The mitochondria were then washed extensively using the following sequence of buffers (at each step, mitochondria were pelleted by centrifugation at 10 000 rpm for 10 min): (a) three washes with 50 mM Tris-HCl/1 mM $MgCl_2$ buffer; (b) one wash with 0.015 M KCl and then three washes with 0.15 M KCl to remove cytochrome *c* and other soluble proteins (Rao and Sanadi, 1960); (c) four to six washes with buffer containing 50 mM Tris-HCl (pH 8.0), 1 mM $MgCl_2$, 50 mM NaCl, and 0.5% fatty acid-free bovine serum albumin; and (d) three washes with buffer containing 50 mM Tris-HCl (pH 8.0), 1 mM $MgCl_2$, 50 mM NaCl, and 1.0 mg/mL dodecyl maltoside (Calbiochem Corp.). The final mitochondrial pellet was suspended to 10 mg/mL protein in this same buffer. This washing procedure results in the loss of about 60–70% of the total protein from the crude mitochondria but in no more than a 10–20% loss of cytochrome *c* oxidase or succinate–cytochrome *c* reductase activity (data not shown).

The washed mitochondrial suspension was stirred gently, and further dodecyl maltoside was added slowly to a final concentration of approximately 1.2 mg of detergent/mg of protein. After being stirred for 15–20 min, the solubilized mitochondria were clarified by centrifugation at 20 000 rpm for 60 min. The clarified detergent extract was adjusted to pH 8.0 and loaded onto a column of DEAE-Biogel (Bio-Rad Corp.) that had been prewashed sequentially with 4.0 M NaCl and 1.0 M Tris-HCl (pH 8.0) and then equilibrated with a buffer containing 50 mM Tris-HCl (pH 8.0), 1 mM $MgCl_2$, 50 mM NaCl, and 0.1 mg/mL dodecyl maltoside. After loading, the column was washed (at least four volumes) with equilibration buffer. Finally, the bc_1 complex was eluted with equilibration buffer in which the NaCl concentration was increased to 400 mM. Pooled fractions containing bc_1 complex (monitored by ferricyanide oxidized/dithionite reduced difference spectra) were then dialyzed overnight against buffer containing 50 mM Tris-HCl (pH 8.0), 1 mM $MgCl_2$, 0.1 mg/mL dodecyl maltoside, 10% glycerol, and 50 mM NaCl.

Using this procedure, it was routinely found that about 50% of the total cytochrome *b* in the detergent extract was

recovered after elution. Electrochemical and spectral analyses of the *b* heme groups in detergent extracts, and in the material that does *not* bind to the anion-exchange column, indicate that most of the unbound heme has a low midpoint potential (about −150 mV) and a reduced absorption maximum of about 559 nm (data not shown). This is probably the *b* heme that is associated with complex II, succinate–ubiquinone oxidoreductase (Ackrell et al., 1992).

The procedure described above is the final version that was adopted after a number of minor variations. The extensive washing procedure is particularly important for good retention of the cytochrome bc_1 complex on the column. Even after this washing procedure, however, the complex from mouse fibroblast mitochondria did not appear to bind as tighly as that from beef heart mitochondria (Ljungdahl et al., 1986). This problem was substantially alleviated by lowering the NaCl concentration from 100 to 50 mM in the column equilibration and loading buffers. We suspect that this problem is due to a higher lipid and/or fatty acid content in mouse fibroblast mitochondria. The eluted complex was found to retain high levels of ubiquinol–cytochrome *c* oxidoreductase activity (data not shown). Using the procedure described here, there was no loss of either cytochrome c_1 or *b* heme groups after storage for 3–4 days at 4 °C. Spectral analysis indicated that the bc_1 complex was contaminated with cytochrome oxidase [see also Ljungdahl et al. (1986)]. To conserve material, however, additional purification steps were not undertaken.

Electrochemical Titrations and Optical Spectroscopy. For the titrations reported here, the cytochrome c_1 concentration was in the range of 5–8 μM. Samples of dodecyl maltoside-extracted and partially purified bc_1 complex were placed in a two-sidearm, side-stirred redox cuvette. An anaerobic atmosphere in the cuvette was maintained by a stream of dry argon. Redox potentials were measured with a Radiometer Model P101 platinum electrode and a Radiometer Model K401 calomel reference electrode standardized against a saturated solution of quinhydrone in 100 mM phosphate buffer (pH 7.0). Details of the methodology may be found in Dutton (1978). Mediation between the electrode, the solution, and the redox centers was achieved using a collection of redox mediator dyes chosen for their electrochemical potentials, their lack of optical interference in the 500–600-nm region, and their ability to mediate effectively in detergent-solubilized preparations of the bc_1 complex. Each titration contained 15 μM 2-hydroxy-1,4-naphthoquinone; 25 μM each of *N*-methyldibenzopyrazine methosulfate, *N*-ethyldibenzopyrazine ethosulfate, phenazine, and pyocyanine; 40 μM each of 1,2-naphthoquinone, 1,4-naphthoquinone, and 1,4-benzoquinone; 50 μM 2,3,5,6-tetramethyl-*p*-phenylenediamine; and 75 μM duroquinone. Mediators were added from stock solutions in dimethyl sulfoxide. At room temperature, the pH of the bc_1 complex plus redox mediators/buffers was about 7.2, a value which consistently dropped to 6.8–6.9 during the course of the electrochemical titration. Since the change in pH is small, no corrections to the E_m values have been made.

During the electrochemical titration, α band electronic absorption spectra of the heme groups were obtained with a dual-wavelength, chopped-beam optical spectrophotometer constructed by the Biomedical Instrumentation Group of the Johnson Research Foundation. At each E_h value, absorbance data were acquired between 510 and 590 nm in 0.4-nm increments using an IBM PC-driven monochrometer and diode detection system. Spectra were taken at E_h intervals of 5 to 25 mV during the reductive titrations. After each addition of reducing or oxidizing agent, 5–10 min was allowed for electrochemical equilibration. Spectral data were acquired, stored, and manipulated using GDATA, a software package developed for this spectrophotometer by the Biomedical Instrumentation Group.

The amount of cytochrome *b* that was reduced at each E_h value was determined as follows. First, a difference spectrum was constructed by subtracting a baseline spectrum taken in which all cytochrome *b* was oxidized (+230 to +250 mV, except in the experiments with funiculosin when a baseline of about +300 mV was used). The amount of cytochrome *b* reduction was then calculated according to the following formula (Rich et al., 1990):

$$[b_{red}] = A_{562} - [(A_{542} + A_{582})/2]$$

The validity of this approach was confirmed in analyses in which the extent of cytochrome *b* reduction was also ascertained from measurement of peak height and from total peak area. These three methods gave identical E_m values with no appreciable differences in the goodness-of-fit. Finally, using the absorbance change at 561 or 563 nm also yielded the same E_m values (data not shown). The extent of cytochrome c_1 reduction was calculated from peak height using a similar approach and with an oxidized baseline spectrum taken at an E_h value of +390–400 mV.

Electrochemical titration data were analyzed with the TANHC software written by Dr. Edward Berry (Lawrence National Laboratories). TANHC provides nonlinear least-squares fits to Nernst functions: the fixed parameters are the number of components and the electrochemical *n* values. The results of the redox titrations were plotted using the RDPLOT software (provided by Drs. Steve Meinhardt and Tomoko Ohnishi, University of Pennsylvania). Deconvolution of the electrochemical titration of the cytochrome *b* heme groups was performed with the number of species fixed initially at two and the *n* values varied until the goodness-of-fit was maximized. The number of components was then increased and the fitting procedure repeated until an overall best fit was obtained. For example, in the reductive titration shown in Figure 6, 36 individual spectra were obtained but five were omitted from analysis due to nonequilibrium (−36, −48, −59, −72, and −87 mV). With the initial parameters set to two components (*n* values of 1.0), the derived E_m values were +183 and −14 mV with an rms error of 3.36×10^{-3}. There was no better fit with three components and *n* values of 1.0. The rms error dropped to 9.69×10^{-4} with four components and *n* values of 1.0, the E_m values being +189, +81, −22, and −148 mV. However, when the *n* value of the highest potential component was set to 0.90 (the others remaining at 1.0), the rms error dropped to 8.10×10^{-4} with E_m values of +187, +49, −25, and −150 mV. Further changes in the *n* values yielded higher rms errors (data not shown), whereas increasing the number of components did not produce any further improvement in the goodness-of-fit.

Spectra of the individual heme groups were obtained by choosing the appropriate E_h regions for reduced–oxidized difference spectra with minimal spectral contamination from other heme groups. This usually involved a 70–100-mV span for the cytochrome *b* heme groups: in all cases, the difference spectra used data from E_h values at which electrochemical equilibrium had been reached (see below). For spectral deconvolution, data from difference spectra were ported into PEAKFIT, a software package (Jandel Scientific Co.) that carried out a nonlinear, least-squares fitting to chosen confidence intervals using mathematical approximations of spectral line shapes. The difference spectra were deconvoluted into a background baseline and a series of Voigtian peaks that corresponded to the previously observed α and β absorption

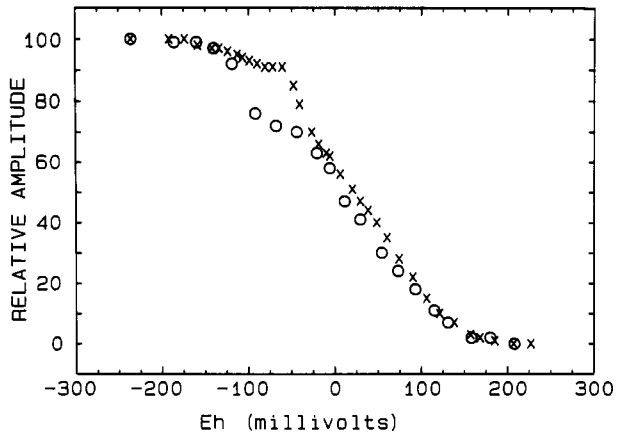

FIGURE 2: Electrochemical titration of the cytochrome *b* heme groups in the partially purified bc_1 complex: (×), data points obtained during titration in the reductive direction; (○), data points obtained during titration in the oxidative direction. Note the region of non-Nernstian electrochemical behavior in the E_h region between 0 and −100 mV.

bands of the heme groups. The goodness-of-fit was uniformly excellent with r^2 values greater than 0.99 (see the caption to Figure 3 for an example).

Chemicals. Antimycin, *N*-methyldibenzopyrazine methosulfate, and *N*-ethylbenzopyrazine ethosulfate were purchased from Sigma. Duroquinone, 2-hydroxy-1,4-naphthoquinone, and 2,3,5,6-tetramethyl-*p*-phenylenediamine were obtained from Aldrich. Pyrocyanine was synthesized by photooxidation of *N*-methyldibenzopyrazine methosulfate and subsequently purified by chloroform extraction. Myxothiazol and stigmatellin were purchased from Fluka. Dodecyl maltoside was purchased from Calbiochem, whereas all other chemicals were obtained from commercial sources.

RESULTS

Properties of the Heme Prosthetic Groups in the Absence of Inhibitors. The rationale of this study was to analyze the long-range interactions among the redox prosthetic groups of the bc_1 complex using electrochemical analysis and high-resolution spectral deconvolution techniques. This approach required an optically clear and concentrated preparation of the bc_1 complex that is obtainable only after detergent solubilization and partial purification. It was necessary, therefore, to demonstrate that this preparation was structurally and functionally native, particularly the heme prosthetic groups. Not only was this requirement met but the high-resolution spectral analyses revealed some previously unrecognized properties of the cytochrome *b* heme groups.

An electrochemical titration of the cytochrome *b* heme groups in the partially purified bc_1 complex is shown in Figure 2. There was non-Nernstian behavior in the E_h region between −100 and 0 mV for both the reductive and oxidative directions of titration. This was a consistent feature of the titrations with dodecyl maltoside-solubilized bc_1 complex and may also be observed in the redox titrations of other investigators [*e.g.*, Figure 4 of Dutton et al. (1970) and Figure 1 of Rich et al. (1990)]. This non-Nernstian behavior was probably not a simple kinetic problem of failing to reach electrochemical equilibrium, as increasing the time after addition of reducing (or oxidizing) agent from 5 to 25–30 min did not remedy the situation (data not shown).[4] The non-Nernstian points were omitted from the data-fitting steps, although it should be noted that most of the points in the reductive titration were within 2–6% of the expected, equilibrium value. The worst points were within 10% of the expected values.

Upon deconvolution, the electrochemical titration data consistently indicated the presence of *four* species of cytochrome *b* heme groups in the partially purified bc_1 complex, two major and two minor. In the reductive titration shown in Figure 2, the two major cytochrome *b* heme groups had E_m values of −33 and +78 mV and represented the b_L and b_H hemes, respectively. Each of these species comprised about 45% of the total cytochrome *b*. A minor, very low potential species (E_m about −150 to −160 mV), accounting for about 5–6% of the total *b* heme, was also observed. This low-potential component was present at higher concentrations in the detergent extracts prior to anion-exchange chromatography (data not shown), and it was probably the remaining cytochrome b_{560} from complex II [see also West et al. (1988)]. Finally, a very high potential form of cytochrome *b* accounted for about 3–4% of the total cytochrome *b*. This species was probably the b_{150} species observed by other investigators and that comprises the fraction of b_H hemes with oxidized quinone bound at the Q_i center (Rich et al., 1990). The concentration of the b_{150} species was low because these titrations were carried out at about pH 7, conditions that did not favor its formation (Rich et al., 1990). Second, the anion-exchange chromatography appears to effectively "strip" the bc_1 complex of lipid and quinone. The b_{150} species is also absent, or nearly so, in the *Rhodobacter* bc_1 complex that has been purified using this method (Robertson et al., 1993). These two minor species are not discussed further in this report.

A consistent feature of the electrochemical titrations was that the best-fit midpoint potentials for the two major cytochrome *b* heme groups consistently required Nernstian *n* values *less than 1* (the number of electrons being transferred during reduction or oxidation). For example, the best-fit E_m values for the reductive titration in Figure 2 were obtained when the *n* values for the b_H and b_L heme groups were set at 0.90 and 0.90, respectively (see also Tables I and II). This

Table I: Spectral and Electrochemical Properties of the Cytochrome b_H Heme Group

exptl condition	E_m[a]	*n*	max	FWHH
control-1[b]	+111	0.85	561.6	9.4
control-2	+94	0.70	561.6	9.3
control-3	+85	0.75	561.3	9.7
control-4	+78	0.90	561.6	9.3
mean (±SD)	+92 (14)	0.80(0.1)	561.5(0.2)	9.4(0.2)
ant	↓20–40[c]	0.85	562.4	9.7
fun	↑90–120	0.90	560.4	8.8
myx	↑15–25	0.80	561.5	10.3
stg	no	0.70	561.7	8.8
ant + myx	↓20	0.85	563.3	10.3
ant + stg	↓30	0.85	562.8	8.8
fun + myx	↑110	0.90	561.2	9.3
fun + stg	↑90	0.90	562.0	8.8

[a] E_m = midpoint potential expressed in millivolts; *n* = the Nernstian *n* value, which is the number of electrons transferred during reduction (see Results); max = reduced absorption maximum in nanometers; FWHH = full widths at half-peak height in nanometers. [b] Control = no inhibitor; ant = antimycin; fun = funiculosin; myx = myxothiazol; stg = stigmatellin. [c] For the redox titrations in the presence of cytochrome *b* inhibitors, we denote the *change* in E_m value rather than the E_m value itself. The ↑ symbol denotes an increase in E_m; ↓ denotes a decrease in E_m; "no" denotes no detectable change in the E_m value.

[4] Using cyclic voltammetry, Mandal and Nair (1991) have observed that ferricyanide anion is sequestered within cationic detergent micelles and is no longer in electrochemical equilibrium with the electrode. Although dodecyl maltoside is a neutral detergent, one or more of the low-potential redox mediators may show a differential distribution between the hydrophobic detergent micelles, or the bc_1 complex itself, and the aqueous phase surrounding the platinum electrode and thereby provide a likely explanation for the nonequilibrium electrochemical behavior. This problem is often ameliorated when the NaCl concentration is raised or in the presence of an inhibitor (data not shown).

nonideal electrochemical behavior suggests that the electronic or electrostatic environments of the two major *b* heme groups are slightly variable as a result of protein flexibility and structural heterogeneity. The best-fit E_m values, therefore, are *population* averages and are analogous to inhomogeneous broadening of absorption spectra (see below). Heterogeneity of the electronic environments of the cytochrome *b* heme groups was first deduced by Salerno (1984), who concluded that the broadened EPR signals of the cytochrome *b* heme groups reflected a range of protein conformations that, in turn, produced a distribution of *g* values [see also the recent EPR studies of Bizzari and Cannistrara (1992) and of Fan et al. (1993)]. Previous studies have not taken this structural heterogeneity into account and have deconvoluted their electrochemical titrations assuming Nernstian *n* values of unity [*e.g.*, Rich et al. (1990)].

In the oxidative titration shown in Figure 2, the E_m values for the cytochrome b_H and b_L heme groups were +77 and −29 mV, values identical to those obtained from the reductive titration, but the *n* values were 0.65 and 0.80. The reductive titration was carried out first, and the total time of these experiments was 4–5 h. The solubilized bc_1 complex is probably changing slowly under these conditions with a resulting increase in structural heterogeneity. For the sake of consistency, only the results from reductive titrations of the cytochrome *b* heme groups are reported in this study.

The α and β band electronic absorption spectra[5] of the reduced cytochrome b_H and b_L heme groups are shown in Figure 3 along with the component transitions obtained after deconvolution. Voigt functions, weighted heavily toward Gaussian character rather than to the Lorentzian component, were found to provide the best fit to optical spectra in the α band region. Best fits for the b_H heme group was obtained with five Voigtian functions: the α band peak, three β or vibronic bands, and a fifth peak that we assign to a small contribution from the α band spectrum of the reduced cytochrome c_1 heme on the basis of its reduced absorption maximum of 553 nm. The spectrum of the cytochrome b_L heme group was also consistenly deconvoluted into five Voigtian functions: two α band absorption peaks and three β band or vibronic peaks.[6] The spectral parameters for the two cytochrome *b* heme groups are summarized in Tables I and II. The vibronic or β absorption bands of both heme groups are uninformative due to their low concentration (about 10% of the total peak area) and are not discussed further.

This is the first study in which the *b* heme oxidized-minus-reduced difference spectra have been deconvoluted, and the results obtained for the "split" α band spectrum of the b_L heme were particularly striking. It was consistently and unambiguously observed that the higher energy transition, which has previously been described as a shoulder on the blue side of the main peak, is more intense than the lower energy transition. Relative peak areas were about 4:1 (Table II).

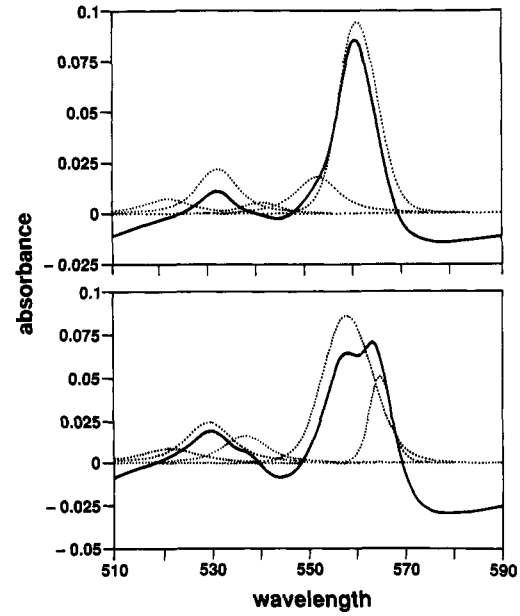

FIGURE 3: Reduced-minus-oxidized α band difference spectra of the reduced b_H (top) and b_L (bottom) heme groups in the bc_1 complex; the E_h spans were +76/+145 and −81/−5 mV, respectively. The solid lines are the raw spectra, while the dotted lines are the Voigtian functions obtained after deconvolution and baseline correction. In the spectrum of the b_H heme, five Voigtian peaks were obtained after deconvolution with the following maxima: 520.4, 532.4, 542.0, 552.0, and 561.6 nm. The first three are the β or vibronic components, the fourth is contamination from the cytochrome c_1 heme, and the fifth is the α band transition of the b_H heme. The standard error of the curve fitting was 0.001 52, while the r^2 value was 0.998. For the b_L heme, the five Voigtian peaks had maxima of 520.6, 529.4, 536.9, 558.1, and 565.2 nm; the first three vibronic components, whereas the latter two are the α band transitions. For this deconvoltion, the standard error of the curve fitting was 0.003 16, while the r^2 value was 0.994.

Inhomogeneous broadening of the cytochrome *b* heme spectra would explain the better fits to Voigtian functions weighted to the Gaussian component. To test this possibility, a series of difference spectra constructed with narrow E_h ranges was analyzed (Table III). For the b_L heme group, the spectral parameters of the lower energy α peak for the b_L heme were relatively constant, but the higher energy transition blue-shifted and narrowed as the E_h window was shifted to more negative values. Preliminary analyses of the b_H heme showed a similar E_h-dependent shift in spectral parameters (data not shown). Therefore, the EPR (Salerno et al., 1984), electrochemical, and absorption spectral analyses all indicate the presence of a structural heterogeneity affecting the *b* heme group environments.

Analysis of four independent preparations of bc_1 complex established that the detergent solubilization and partial purification procedures yielded satisfactorily reproducible results (Table I and II). The E_m values show the greatest variability, although they are in good agreement with those obtained with membranously intact bc_1 complex. For example, in recent studies of beef heart SMP, Rich et al. (1990) found that, at pH 7.0, the E_m values for the b_H and b_L heme groups were +95 and −20 mV, respectively. As a rule-of-thumb for the inhibitor titrations, it was unlikely that E_m shifts less than 20 mV and spectral shifts less than 0.3 nm were significant.

In addition to the cytochrome *b* heme groups, the cytochrome c_1 heme group has also been analyzed. In the bc_1 preparation used for the experiment shown in Figure 2, an E_m value of

[5] The α band spectra of heme groups are also designated Q_o, but the former term is used here to avoid confusion with the quinol oxidizing center of the bc_1 complex. Similarly, the β or vibronic transitions are also designated as the Q_v absorption bands.

[6] Due to the difference in the E_m values of the two cytochrome *b* heme groups, the spectrum of the reduced b_H heme group is always obtained here when the b_L heme is oxidized, while that of the reduced b_L heme is derived under experimental conditions in which the b_H heme is reduced. West et al. (1988) were able to obtain the spectrum of the reduced b_L heme group when the b_H heme was *oxidized* and reported no significant differences from that obtained under the standard experimental conditions. More recently, Yun et al. (1991) have shown that removal of the b_H heme group through site-directed mutagenesis has only a slight effect upon the spectrum of the b_L heme group. It thus appears that the spectrum of a cytochrome *b* heme is not influenced by the redox status of the other.

Table II: Spectral and Electrochemical Properties of the Cytochrome b_L Heme Group

exptl condition	E_m[a]	n	max$_1$	FWHH$_1$	area$_1$	max$_2$	FWHH$_2$	area$_2$
control-1[b]	−20	0.85	558.1	11.8	0.71	565.2	6.5	0.29
control-2	−23	0.75	558.2	13.7	0.86	565.2	5.4	0.14
control-3	−46	1.0	558.6	13.2	0.81	565.2	5.4	0.19
control-4	−33	0.90	559.2	13.7	0.85	565.2	5.4	0.15
mean (±SD)	−31(12)	0.88(0.1)	558.5(0.5)	13.1(0.9)	0.81(0.1)	565.2(0)	5.6(0.6)	0.19(0.1)
ant[b]	↓20[b]	1.2	559.2	12.7	0.81	564.9	5.4	0.19
fun	↑10–20	1.0	557.8	11.3	0.68	565.2	5.7	0.32
myx	↑10–30	1.0	558.6	13.7	0.78	565.5	6.6	0.22
stg	no	1.0	558.6	13.7	0.77	566.0	5.4	0.23
ant + myx$_1$[c]	↑20–30	1.0	559.0	10.9	0.60	564.8	7.7	0.40
ant + myx$_2$	no	1.0	558.0	12.6	0.72	564.8	8.5	0.28
ant + stg	↓20	1.0	559.1	14.6	0.80	566.5	6.3	0.20
fun + myx$_1$[d]	↑70	1.0	558.8	12.3	0.62	566.4	5.5	0.38
fun + myx$_2$	no	1.0	558.0	14.1	0.86	566.0	5.9	0.14
fun + stg	↑20	1.15	558.8	13.7	0.78	566.8	5.9	0.22

[a] Symbols are defined as in Table I with the addition of the fractional areas of the two α band peaks. [b] See Table I. [c] The ant + myx$_1$ spectrum was constructed from a −29/−1-mV E_h span, and the ant + my$_2$ spectrum was from a −84/−38-mV E_h span. [d] The fun + myx$_1$ spectrum was constructed from the +35/+6-mV E_h span, and the fun + myx$_2$ spectrum was from the 48/−25-mV E_h span.

Table III: Spectral Changes in the Cytochrome b_L Heme Group as a Function of E_h

E_h window[a]	max$_1$	FWHH$_1$	area$_1$	max$_2$	FWHH$_2$	area$_2$[a]
−81/−5[b]	559.2	13.7	0.85	565.2	5.4	0.15
−20/−3	559.7	12.7	0.81	565.2	5.4	0.19
−29/−5	559.2	12.3	0.78	565.2	5.4	0.22
−36/−13	558.6	12.7	0.77	565.2	5.4	0.23
−46/−20	558.6	11.7	0.76	565.2	5.4	0.24
−53/−29	558.9	12.7	0.82	565.2	4.9	0.18
−84/−36	558.1	10.7	0.79	564.6	4.9	0.21

[a] The E_h window is the range (in mV) used for construction of the difference spectra and subsequent deconvolution. The spectral parameters are defined as in Table II. [b] This is the same spectrum as control-4 in Table II.

+236 mV (n = 1.0) and a reduced absorption maximum of 553.2 nm were found.

Finally, experiments have shown that the spectral and electrochemical properties of the heme prosthetic groups are relatively insensitive to the medium in which the titrations were performed. For example, varying the salt concentration (reduced to 0 or increased to 250 mM NaCl) produced only subtle changes in the spectral characteristics of the cytochrome b heme groups with no effects upon the E_m values (data not shown). Increasing the concentration of dodecyl maltoside to 10 mg/mL (the concentration used for membrane solubilization) also produced only subtle changes in the spectral parameters. Most importantly, the effects of the cytochrome b inhibitors are essentially the same at the higher NaCl concentration (data not shown).

Effect of Single Cytochrome b Inhibitors upon the Heme Prosthetic Groups. The major aim of these experiments was to ascertain if inhibitors that bind at one redox site, Q_o and Q_i, alter the electrochemical and spectral properties of the distal cytochrome b heme group. The results summarized in Tables I and II show that all four inhibitors affect the spectral properties of the distal heme group. In contrast, inhibitor binding has little, if any, effect upon the E_m of the distal heme, even in cases where there is a large shift in that for the proximal heme. Previous studies have made some of the same observations but at a lower level of resolution (Tsai & Palmer, 1982; Kunz & Konstantinov, 1983; Kamensky et al., 1985; Rich et al., 1990).

Inhibitor Effects on the b_H Heme Group. The effects upon the cytochrome b_H heme group of the Q_i inhibitors antimycin and funiculosin and of the Q_o inhibitors myxothiazol and stigmatellin are summarized in Table I and Figure 4. The

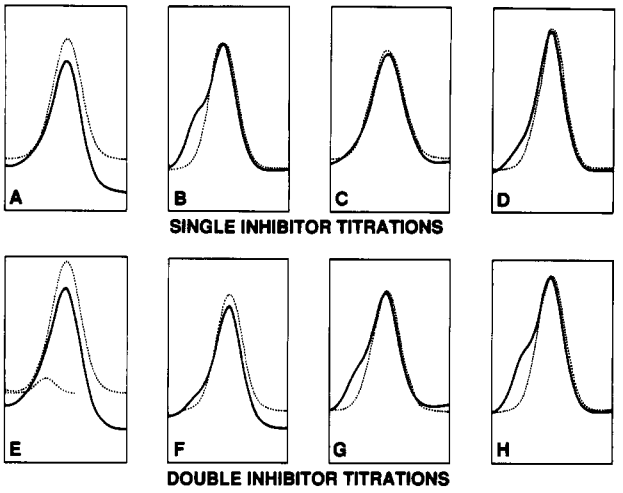

FIGURE 4: Influence of inhibitors upon the spectrum of the b_H heme group. In each panel, the solid line is the raw spectrum, while the dotted line is the Voight function obtained after deconvolution and baseline correction. The contamination of the spectrum by the c_1 heme group accounts for the shoulder on the blue side of the spectrum; the corresponding Voigt function is omitted to emphasize the line shape of the b_H optical transitions. A, antimycin; B, funiculosin, C, myxothiazol; D, stigmatellin; E, antimycin and myxothiazol; F, antimycin and stigmatellin; G, funiculosin and myxothiazol; H, funiculosin and stigmatellin. The spectra used for deconvolution typically involved difference spectra from the range of +60 to +140 mV except in the presence of funiculosin when the range was +140 to +220 mV. Note that, in the presence of antimycin and myxothiazol, an additional peak around 558 nm was obtained during spectral deconvolution.

results demonstrate that the latter induce significant changes in the spectrum of this heme group, despite the intervening distance of the membrane dielectric between the Q_o site and this heme group (Figure 1).

The Q_i inhibitor antimycin induced a red shift in the reduced absorption maximum of the b_H heme (von Jagow & Link, 1986) and induced a slight broadening of the spectrum. Funiculosin, another Q_i inhibitor, had markedly different effects upon the b_H heme group: it raised the E_m by about 100 mV and induced a blue shift in the reduced absorption maximum. The high-resolution analysis also indicated that there was a narrowing of the spectrum, a finding not reported previously.

The Q_o inhibitor stigmatellin did not alter the E_m or the reduced absorption maximum of the b_H heme group, although it narrowed the spectrum. Hauska et al. (1989) reported both a small increase in the E_m and a narrowing of the b_H spectrum.

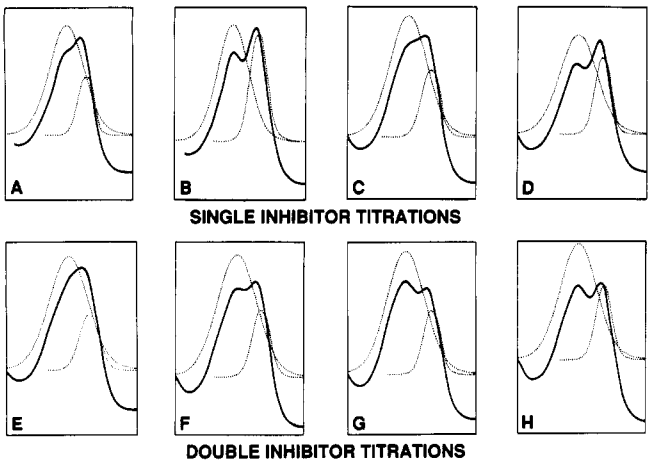

FIGURE 5: Influence of inhibitors upon the spectrum of the b_L heme group. In each panel, the solid line is the raw spectrum, while the dotted lines are the two Voight functions obtained after deconvolution and baseline correction. The inhibitors used for the spectra in panels A–H are the same as those used for the spectra in Figure 4. The spectra used for deconvolution typically involved difference spectra from the range of −100 to −10 mV.

Myxothiazol, another Q_o inhibitor, raised the E_m of this heme group by 15–25 mV and increased the spectral width.

Inhibitor Effects on the b_L Heme Group. In parallel with the findings of the previous section, inhibitors that bind at the Q_i site induced changes in the spectrum of the b_L heme group (Table II and Figure 5). Thus, in the presence of antimycin, the width of the higher energy α band component was narrowed while the lower energy component showed a small blue shift, with the cumulative effect being a narrowing of the unresolved spectrum. For funiculosin, in contrast, the higher energy component of the deconvoluted α band spectrum showed a pronounced narrowing and blue shift while the lower energy component was slightly broadened. Furthermore, the relative areas of the two α band peaks showed a marked shift (Table II). This effect cannot be explained by reduced spectral contamination from the b_H heme.

Stigmatellin induced subtle spectral changes through a red-shifting of the higher energy α band transition and a change in the relative areas of the two peaks. Hauska et al. (1989) concluded that stigmatellin induced a red shift in the b_L spectrum and a *decrease* in the splitting of the two component peaks. However, inspection of their spectra indicates an *increase* in the separation of the two α band transitions, a result compatible with our observations (see their Figure 7).

Myxothiazol produced a small increase in the E_m of the cytochrome b_L heme group, results in agreement with those of Rich et al. (1990) and Kunz and Konstantinov (1983). Meinhardt and Crofts (1982) also found that myxothiazol raises this E_m in the bc_1 complex from the prokaryote *Rhodobacter sphaeroides*. This inhibitor had relatively subtle effects upon the b_L heme: a broadening of the lower energy peak and a lower area ratio of the two α band transitions. Rich et al. (1990) and Meinhardt and Crofts (1982) reported small blue shifts of this heme by myxothiazol, but deconvolutions of the reduced b_L spectrum were not reported, so it is not possible to compare our results with theirs.

The effects of myxothiazol upon the α band spectra of the cytochrome b_H and b_L heme groups are a good illustration of the confusion that can arise when low-resolution spectral studies are carried out. In previous studies with this inhibitor, some investigators have reported a red shift of the b_L spectrum (von Jagow & Link, 1986), while others (see above) have reported a blue shift. When we constructed a simple, fully reduced +myx/−myx difference spectrum, there was a "trough" at about 558 nm and a "peak" at about 567 nm (data not shown). This difference spectrum thus had the characteristics of a simple red shift of the b_L heme group. However, our spectral deconvolutions demonstrate that this simple pattern is actually the combined effect of myxothiazol upon *both* cytochrome *b* heme groups. The reports of a simple stigmatellin-induced red shift in the b_L heme spectrum (von Jagow & Link, 1986) must be treated with similar caution (data not shown).

Cytochrome c_1 Heme Group. None of these inhibitors, when present singly, was found to detectably alter the E_m or spectral characteristics of the cytochrome c_1 heme group (data not shown).

Results of Q_i Plus Q_o Double-Inhibitor Redox Titrations. To address further the long-range effects of inhibitor binding upon the bc_1 complex, a series of titrations were carried out in which both a Q_o and a Q_i inhibitor were present. The clear trend was that tight binding of an inhibitor at the proximal quinone site (in the sence of association with the b_H or b_L heme group) did *not* negate the effects of inhibitor binding at the distal site. Both additive and nonadditive effects were observd, particularly for the spectral characteristics of the cytochrome *b* heme groups.

Effects of a Q_o Inhibitor on the b_H Heme Group. The results in Table I and Figure 4 summarize the effects of a Q_o inhibitor upon the cytochrome b_H heme group when there was an inhibitor, antimycin or funiculosin, simultaneously occupying the Q_i site. The effects of Q_i inhibitors on the E_m values of the b_H heme were not attentuated or potentiated by a Q_o inhibitor. However, in all cases, binding of an inhibitor at the Q_o site changed the spectrum of the b_H heme when an inhibitor was also bound at the Q_i center.

The red shift of the b_H spectrum induced by antimycin has already been noted. When both antimycin and myxothiazol were present, the red shift was much larger, almost 2 nm, and the spectrum was broadened (Table I). However, the increase in spectral width was not symmetrical, but instead, spectral deconvolution indicated a second α band with a maximum at about 558 nm (Table I). This band is independent of the spectral contamination from the cytochrome c_1 heme group, as shown by deconvolution of spectra taken at different E_h spans to reduce the amount of residual c_1 absorption (data not shown). Myxothiazol alone broadened the spectrum of the b_H heme (Table I), but due to the greater overlap of the c_1 and b_H spectra under these conditions, it was not clear if the broadening was symmetrical or due to an additional absorption band on the blue side of the main peak.

The anitmycin-induced red shift was also enhanced when stigmatellin was present. Additionally, stigmatellin markedly narrowed the b_H spectrum, and this effect was maintained even when antimycin occupied the Q_i center. This is an example of a b_H heme property for which the Q_o inhibitor was dominant over the Q_i inhibitor. As shown in Table I, both Q_o inhibitors eliminated the funiculosin-induced blue shift in the reduced absorption maximum of the cytochrome b_H heme.

Effects of a Q_i Inhibitor upon the b_L Heme Group. When stigmatellin was bound at the Q_o site, the effects of a Q_i inhibitor were relatively straightforward (Table II). As noted earlier, stigmatellin alone widened the separation between the two α band optical transitions through red-shifting of the lower energy transition. Both antimycin and funiculosin enhanced this effect of stigmatellin, with the former also broadening the width of both transitions (Figure 5). The similar effects of the two Q_i inhibitors, when stigmatellin was bound, were interesting since antimycin and funiculosin have substantially different effects on the b_L spectrum in the absence

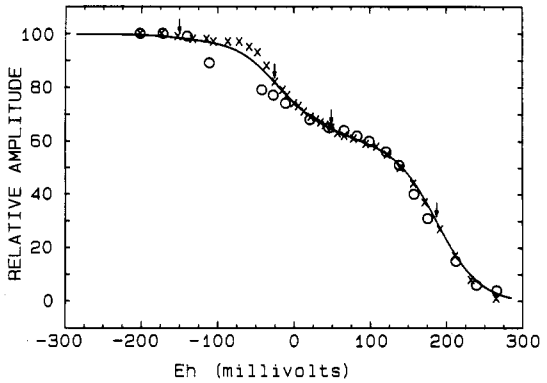

FIGURE 6: Electrochemical titration of the cytochrome *b* heme groups in the presence of funiculosin and myxothiazol: (×), data points obtained during titration in the reductive direction; (○), oxidative titration. The solid line is the fitted curve based upon analysis of the reductive titration data (the five points not in equilibrium were excluded; see the Materials and Methods section for further details). The best fit was obtained with *two* species of b_L heme, one b_H species, and a small amount of a fourth, very low potential component. The derived E_m (n) values in mV were +189 (0.90), +81 (1.0), −22 (1.0), and −148 (1.0) with a rms error of 8.10×10^{-4}; these values are indicated here by vertical arrows.

of a Q_o inhibitor (Table II). The small increase and the small decrease in the E_m value in the presence of funiculosin and antimycin, respectively, were not changed when stigmatellin was bound at the Q_o site.

The results obtained in the double-inhibitor experiments involving myxothiazol were particularly striking. In the double-inhibitor titration with antimycin and in that with funiculosin, there were *two* spectrally and electrochemically distinct species of the b_L heme group. The presence of two b_L species was most clearly seen in the experiment with myxothiazol and funiculosin since the E_m values, −25 and +50 mV, were well-separated (Figure 6 and Table II) and reasonably "pure" spectra of the two b_L species could be obtained (Figure 7). The spectrum of the higher potential form showed to relatively widely separated and narrow α band peaks; the relative intensity of the lower energy transition was the greatest for any of the conditions used in these studies. In contrast, the species with the lower E_m value was dominated by a broad and very intense α band centered at 558 nm (Table II).

There was also evidence for two species of the b_L heme in the presence of antimycin and myxothiazol, although it came more from the spectral analyses than from the electrochemical data. There were marked differences in the b_L spectrum as a function of the E_h span (Table II and Figure 7), differences that were obviously greater than the variation seen in the absence of inhibitor (Table III). In view of the results described above, we deconvoluted the electrochemical titration in terms of two species of b_L heme. The redox titration data were compatible with a single b_L species with an E_m value of about −20 mV. West et al. (1988) also obtained an E_m value of −20 mV for this group heme in the presence of antimycin and myxothiazol. However, a slightly better fit was obtained if we assumed two b_L species with n values of unity and E_m values of 0 and −30 mV. Since the E_m values of the two putative b_L species were so close, clearly resolved spectra were not obtainable, but as was found for the funiculosin plus myxothiazol experiment, the putative b_L species with the lower E_m value had a more predominant higher energy component (Table II and Figure 7).

Effects upon the Cytochrome c_1 Heme Group. There were preliminary indications that the properties of the cytochrome c_1 heme group were altered in some of the double-inhibitor

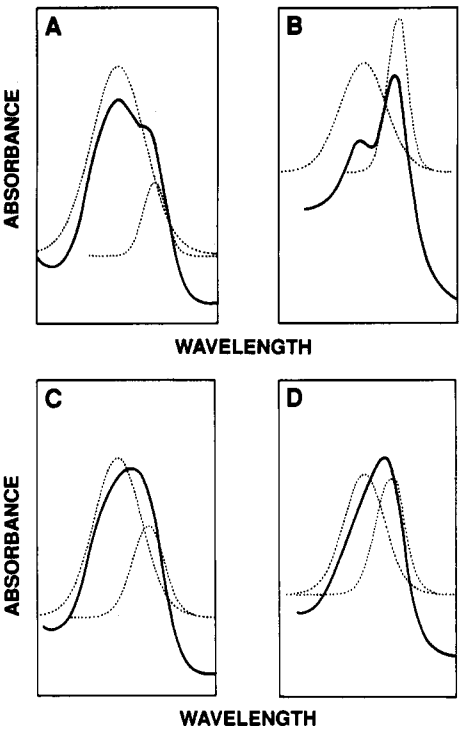

FIGURE 7: Spectral evidence for two species of the b_L heme group in the presence of myxothiazol and funiculosin (panels A and B) and myxothiazol and antimycin (panels C and D). In each panel, the solid line is the raw spectrum, while the dotted lines are the two Voight functions obtained after deconvolution. For the electrochemical titration involving myxothiazol and funiculosin, the E_h spans used for spectral deconvoltion were −48/−25 mV (A) and +6/+35 mV (B). The E_h spans for the titration with myxothiazol and antimycin were −84/−38 mV (C) and −29/−1 mV (D).

experiments. Thus, the reduced absorption maximum of this heme was red-shifted to 553.7 nm in the experiment involving funiculosin and stigmatellin. Furthermore, the E_m value of this heme group may have been increased by about 20–30 mV in both the funiculosin plus myxothiazol and the funiculosin plus stigmatellin experiment. As this heme group has not been analyzed as extensively as the cytochrome *b* heme groups, these findings are less robust, and additional studies are underway.

ANALYSIS AND CONCLUSIONS

These electrochemical and spectral analyses of the heme prosthetic groups of the bc_1 complex are the most comprehensive studies carried out thus far, particularly with regard to the effects of inhibitors which bind at the Q_i and Q_o sites. The general conclusion is that the inhibitors antimycin, funiculosin, myxothiazol, and stigmatellin, irrespective of whether they bind at the Q_o or the Q_i site, alter the spectra of the distal *and* the proximal *b* hemes. In contrast, only funiculosin induces a large change in E_m, and that is for the proximal *b* heme. The high-resolution spectral analyses encouarge us to interpret the results in terms of the standard orbital model for heme compounds and, on the basis of this, to make additional suggestions about the structure–function relationships within the proton-motive cytochrome *b* protein.

Several factors may influence the E_m value of heme groups in cytochromes, including the apolarity/hydrophobicity of the environment around the heme group (Kassner, 1972), the degree of solvent exposure of the heme group (Stellwagen, 1978), the charges of the heme macrocycle propionic acid groups (Moore, 1983; Lee et al., 1991), the strength of the hydrogen bond between the histidine ligand and a protein backbone carbonyl group (Valentine et al., 1979; Desbois &

Lutz, 1992; Goodin & McRee, 1993), and the electrostatic environment around the heme group established by the charged or polar amino acid side chains of the protein (Eccles & Honig, 1983). From an analysis of the tetraheme cytochrome associated with the *Rhodopseudomonas viridis* reaction center, Gunner and Honig (1991) concluded that the major factor controlling the E_m values of the heme groups was the electrostatic interactions with the polar and ionizable moieties of local amino acid residues.

The optical spectra of cytochrome heme groups have been the subject of intense investigation [reviewed in Gouterman (1978), Makinen and Churg (1983), and Moore and Pettigrew (1990)]. According to the four-orbital model of Gouterman (1961) for hemes of D_{4h} point-group representation, the HOMO a_{1u} and a_{2u} π bonding orbitals of the heme macrocycle show a strong configuration interaction and are nearly degenerate. Excitation of an electron to a LUMO e_g antibonding π^* orbital thus results in a strongly allowed transition (the Soret or *B* band) and a weakly allowed transition (the α or Q band). The α band is not always a pure π–π^* transition but may involve contributions from the heme iron d orbitals [*e.g.*, the studies on deoxymyoglobin of Bangcharoenpaurpong et al. (1984)]. The π–π^* transitions result in the effective movement of electrons toward the periphery of the heme macrocycle. As a result, increasing the electron-withdrawing character of the environment at the edge of the macrocycle will result in a red shift of the optical transition (*viz*, less energy is required to excite the electron to the higher orbital). Conversely, increasing the electron-donating character will produce a blue shift (Moore & Pettigrew, 1990). Unfortunately, there is little ability, at present, to interpret spectral shifts quantitatively in terms of heme group structure.

In the studies presented here, several instances were observed in which spectral width was increased or decreased as a consequence of inhibitor binding. Spectral width is a complex function which is determined by any of several factors, including torsions of the histidine–iron ligands, librations of the heme, heme doming motions (these factors are unlikely to be relevant here, as the cytochrome *b* heme groups have two axial ligands), histidine tilt and azimuthal orientation, inhomogeneous broadening due to multiple protein conformations, rate of nonradiative decay (homogeneous broadening), and changes in the x–y degeneracy of the heme group (Friedman et al., 1977; Andrews et al., 1981; Schomacker & Champion, 1986; Srajer et al., 1986). In at least some cases, inhibitor binding apparently alters x–y degeneracy, presumably through changes in protein conformation that affect the structural anisotropy of the electrostatic or electronic environment around the heme groups. This is most strongly indicated from the spectral analyses of the b_L heme in which the degree of splitting between the two α band transitions is increased or decreased (Table II). Although the b_H heme does not show α band splitting at room temperature, lifting of x–y degeneracy could also underlie changes in the spectral width of the b_H heme. Thus, in the presence of antimycin and myxothiazol, the b_H heme is broadened considerably, and the deconvolution analysis suggests the presence of a second α band transition around 558 nm, the behavior expected if x–y degeneracy is decreased (Figure 4E). Conversely, the narrowing of the b_H spectrum induced by funiculosin and stigmatellin (Table I) is most easily explained by an increase in the imperfect degeneracy of the a_{1u}–e_g and a_{2u}–e_g transitions.[7]

The deconvolution of the reduced b_L heme spectrum revealed a previously unrecognized difference in the line shapes of the individual electronic transitions. The higher energy component is clearly much broader and more intense than the lower energy transition (Figure 3); this is true irrespective of the preparation analyzed or the experimental conditions.[8] Shelnutt (1980) has shown that, for a four-orbital model with pure π–π^* transitions, lowering the symmetry from D_{4h} will result in the *lower* transition being more intense, as is the case for different cytochrome *c* proteins at low temperatures. However, Friedman et al. (1977) found that the low-temperature α band spectrum of the cytochrome b_5 heme group had a more intense higher energy transition, and they concluded that the two α band transitions differed in their coupling to nonradiative decay channels (probably iron d orbitals). The changes in the width of the individual transitions of the b_L heme group observed here may also represent changes in the coupling to such channels. Changes in the oscillator strength of the individual electronic transitions cannot be ruled out, however. Unfortunately, since the present analyses are limited to reduced *minus* oxidized spectra, rather than absolute spectra, this issue remains open for the present. Similarly, effects due to changes in tilt and azimuthal orientation of the heme-liganding histidine residues cannot yet be evaluated.

The most striking result obtained in these studies was the detection of two spectrally and electrochemically distinct species of the b_L heme group in the presence of myxothiazol and a Q_i inhibitor. Neither species has the properties characteristic of the b_L heme group in the presence of either inhibitor singly or in the absence of inhibitor (Table II and Figure 5). This is an important point since it indicates that neither of the two b_L species results from a subpopulation of bc_1 complexes in which only a single inhibitor (funiculosin or stigmatellin) is bound, or a subpopulation lacking both inhibitors. These two species may reflect the occurrence of two major conformational substrates under these experimental conditions. It cannot be ruled out that there are two major substrates *in the absence of inhibitor*, but that their spectral and electrochemical properties are identical, or nearly so, until two inhibitors are bound. This possibility is compatible with the electrochemical titrations and could explain the less-than-unity n values that were measured (Tables I and II). The bc_1 complex may function as a heterodimer (de Vries, 1986; Schmitt & Trumpower, 1990; Fernandez-Velasco & Crofts, 1991; Bechmann et al., 1992), and it is tempting to speculate that the presence of two species of the b_L heme observed in these studies is related to a heterodimeric structure of the bc_1 complex.

The two cytochrome *b* heme groups are separated within the membrane dielectric by a considerable distance (Glaser & Crofts, 1984; Konstantinov & Papova, 1987; Robertson & Dutton, 1988). Despite this physical separation, our results indicate that, in the bc_1 preparations used here, each of the four inhibitors tested had long-range effects on the spectra of *both* of the cytochrome *b* heme groups. There was, moreover, preliminary evidence from the double-inhibitor titrations that the properties of the cytochrome c_1 heme were also altered

[7] The width of the α band of the cytochrome b_H heme group is noticeably broader than that of the cytochrome c_1 heme group, about 9.4 *versus* 8.0 nm. We thus suspect that there is some lifting of the x–y degeneracy in the α band transitions for the b_H heme. There is precedence for such behavior, as a slight splitting of the unimodal α band of cytochrome *c* at room temperature is detectable by MCD and polarization dispersion (Sutherland & Klein, 1972; Collins et al., 1976).

[8] Forcing the fitting program to the reverse situation (*viz.*, a more intense lower energy transition) invariably results in a very poor fit when realistic conditions are set. In what is the only other study that deconvoluted the b_L spectrum, Arutjunjan et al. (1978) assumed two Lorentzian transitions of equal half-widths and an intensity ratio of 1:2 for the high- and low-energy components; however, they made no effort to test the fit of the other models.

under some conditions. How might long-range effects of inhibitor binding be transmitted in the bc_1 complex? The two pairs of histidine ligands to the cytochrome b_H and b_L heme groups occur within two parallel transmembrane α-helices (Widger et la., 1984; Link et al., 1986; Howell & Gilbert, 1988). This unusual motif is predicted to occur for the cytochrome *b* proteins of both bc_1 and chloroplast b_6f complexes as well as in at least one bacterial ubiquinol oxidase (Lubben et al., 1992). Modeling studies (R. S. Farid and D. E. Robertson, in preparation) indicate that the distances of each ϵ nitrogen of the histidine ligands from the heme iron atom and the orientations of the histidine imidazole planes are controlled principally by the number of amino acid residues between the ligand pairs, by the relative orientation of the two helical protein segments, and by the hydrogen bonding of the δ nitrogens of the histidine ligands to the protein backbone. One can envision, therefore, a protein conformational change at one end of this heme–helical bundle resulting in spectral changes to both heme groups. In contrast, the *net* change in the sum of the electrostatic contributions from the amino acid side chains to the electrochemistry of the heme groups may be small. Many of these electrostatic interactions may, in fact, be donated by as many as four additional transmembrane helices arranged near the heme–helical bundle. Further evidence for long-range conformational effects comes from the studies of Hacker et al. (1993). Site-directed mutagenesis of highly conserved amino acid residues affecting the function of the Q_i site in the *R. sphaeroides* bc_1 complex produced shifts in the E_m of the distal b_L heme.

Although the changes in the spectra of the cytochrome *b* heme groups are relatively small (1–2 nm), this does not rule out substantial protein conformational effects. In contrast to chlorophyll-containing proteins (Gudowska-Nowak et al., 1990; Fowler et al., 1992), the porphyrin π electrons of cytochrome heme groups are relatively insensitive (*viz.*, weakly coupled) to changes in the protein backbone (Schomacker & Champion, 1986). For example, substitution of the Val68 residue in human myoglobin (which is in van der Waals contact with the heme group) with Glu or Asp results in a decrease in the E_m value of about 200 mV, although the changes in the reduced absorption maxima of the π–π^* transitions are no more than 2 nm (Varadarajan et al., 1989a,b). This same trend can be seen with funiculosin where a 100-mV increase in the E_m of the b_H heme is accompanied by a 0.5-nm blue shift.

The minimal long-range effects of inhibitor binding upon the E_m values of the distal cytochrome *b* (or c_1) heme group suggest that the Q_o and Q_i redox sites may operate independently of one another, at least in the sense that the redox status at one site does not "set" or modify the status at the other. The reasoning underlying this conclusion is as follows: The difference in the E_m values for the two *b* heme groups is about 120 mV, or 2.8 kcal, which should be compared to the 10–20-mV (0.23–0.46 kcal) changes, at most, that are observed in the E_m of the distal heme induced by inhibitor binding (Tables I and II). Considering that these inhibitors bind with such affinity as to displace quinone reactants and intermediates from the reaction sites (von Jagow & Link, 1986), it is unlikely that any conformational changes occurring during catalytic turnover would be greater than those induced by inhibitor binding. This catalytic independence of the Q_o and Q_i sites is compatible with the view that electron-transfer proteins behave as organic glasses and form a uniform electronic "barrier" to electron tunneling (Moser et al., 1992). On the other hand, shorter range interactions may have more functional significance. The sensitivity of the E_m of the b_H heme to the occupancy of the Q_i site (de la Rosa & Palmer, 1983; Salerno et al., 1989; Rich et al., 1990) and that of the FeS center to the occupancy of the Q_o site (Bowyer et al., 1980; Matsuura et al., 1983; von Jagow & Ohnishi, 1985) are well-established and of considerable magnitude (the funiculosin/b_H and stigmatellin/FeS effects represent 2.3 and 4–5 kcal, respectively). Therefore, we suggest that in the Q cycle the Q_o site, the b_L heme group, and the FeS form one unit of redox function, while the Q_i site and the b_H heme form a second.

ACKNOWLEDGMENT

We thank Mian Xu and Iwona Kubacka for their technical assistance. A number of our colleagues made helpful suggestions and offered sound advice during the course of this work, but we particularly acknowledge the contributions of Professor P. L. Dutton.

REFERENCES

Ackrell, B. A. C., Johnson, M. K., Gunsalus, R. P., & Cecchini, G. (1992) in *Chemistry and Biochemistry of Flavoenzymes* (Muller, F., Ed.) pp 229–297, CRC Press, Boca Raton, FL.

Andrews, J. R.; Hochstrasser, R. M., & Trommsdorff, H. P. (1981) *Chem. Phys. 62*, 87–101.

Arutjunjan, A. M., Kamensky, Y. A., Milgrom, E., Surkov, S., Konstantinov, A. A., & Sharoniv, Y. A. (1978) *FEBS Lett. 95*, 40–44.

Atta-Asafo-Adjei, E., & Daldal, F. (1991) *Proc. Natl. Acad. Sci. U.S.A. 88*, 492–496.

Austin, R. H., Beeson, K. W., Eisenstein, L., Frauenfelder, H., & Gunsalus, I. C. (1975) *Biochemistry 14*, 5355.

Bangcharoenpaurpong, O., Schomaker, K. T., & Champion, P. M. (1984) *J. Am. Chem. Soc. 106*, 5688–5698.

Beattie, D. S., Japa, S., Howton, M., & Zhu, Q. S. (1992) *Arch. Biochem. Biophys. 292*, 499–505.

Bechmann, G., Weiss, H., & Rich, P. R. (1992) *Eur. J. Biochem. 208*, 315–325.

Bizzari, A. R., & Cannistrara, S. (1992) *Biophys. Chem. 42*, 79–85.

Bowyer, J. R., & Trumpower, B. L. (1981) in *Chemiosmotic Proton Circuits in Biological Membranes* (Skulachev, V. P., & Hinkel, P. C., Eds.) pp 105–122, Addison Wesley Publishing Co., Reading, MA.

Bowyer, J. R., Dutton, P. L., Prince, R. C., & Crofts, A. R. (1980) *Biochim. Biophys. Acta 592*, 445–460.

Brandt, U., & von Jagow, G. (1991) *Eur. J. Biochem. 195*, 163–170.

Brasseur, R. (1988) *J. Biol. Chem. 263*, 12571–12575.

Collins, D. W., Champion, P. M., & Fitchen, D. B. (1976) *Chem. Phys. Lett. 40*, 416–419.

Crofts, A. R. (1985) in *The Enzymes of Biological Membranes* (Martonosi, A. N., Ed.) Vol. 4, pp 347–382, Plenum Publishing Corp., New York.

Crofts, A. R., Robinson, H., Andrews, K., Van Doren, S., & Berry, E. (1987) in *Cytochrome Systems. Molecular Biology and Bioenergetics* (Papa, S., Chance, B., & Ernster, L., Eds.) pp 617–624, Plenum Press, New York.

Daldal, F., Tokito, M. K., Davidson, E., & Faham, M. (1989) *EMBO J. 8*, 3951–3961.

Degli Esposti, M., Palmer, G., & Lenaz, G. (1989) *Eur. J. Biochem. 182*, 27–36.

de la Rosa, F. F., & Palmer, G. (1983) *FEBS Lett. 163*, 140–143.

Desbois, A., & Lutz, M. (1992) *Eur. Biophys. J. 20*, 321–335.

de Vries, S. (1986) *J. Biomembr. Bioenerg. 18*, 195–224.

Ding, H., Robertson, D. E., Daldal, F., & Dutton, P. L. (1992) *Biochemistry 31*, 3144–3158.

di Rago, J.-P., & Colson, A.-M. (1988) *J. Biol. Chem. 263*, 12564–12570.

di Rago, J.-P., Coppee, J.-Y., & Colson, A.-M. (1989) *J. Biol. Chem. 264*, 14543–14548.

Dutton, P. L. (1978) *Methods Enzymol. 54*, 411–435.
Dutton, P. L., Wilson, D. F., & Lee, C.-P. (1970) *Biochemistry 9*, 5077–5082.
Eccles, J., & Honig, B. (1983) *Proc. Natl. Acad. Sci. U.S.A. 80*, 4959–4962.
Fan, C., Houseman, A. L. P., Doan, P., & Hoffman, B. M. (1993) *J. Phys. Chem. 97*, 3017–3021.
Fernandez-Velasco, J., & Crofts, A. R. (1991) *Biochem. Soc. Trans. 19*, 588–593.
Fowler, G. J. S., Visschers, R. W., Grief, G. G., van Grondelle, R., & Hunter, C. N. (1992) *Nature 355*, 848–850.
Friedman, J. M., Rousseau, D. L., & Adar, F. (1977). *Proc. Natl. Acad. Sci. U.S.A. 74*, 2607–2611.
Furbacher, P. N., Girvin, M. E., & Cramer, W. A. (1989) *Biochemistry 28*, 8990–8998.
Glaser, E., & Crofts, A. R. (1984) *Biochim. Biophys. Acta 766*, 322–333.
Goodin, D. B., & McRee, D. E. (1993) *Biochemistry 32*, 3313–3324.
Gouterman, M. (1961) *J. Mol. Spectrosc. 6*, 138–161.
Gouterman, M. (1978) in *The Porphyrins. Volume III. Physical Chemistry, Part A* (Dolphin, D., Ed.) pp 1–165, Academic Press, New York.
Gudowska-Nowak, E., Newton, M. D., & Fajer, J. (1990) *J. Phys Chem. 94*, 5795–5801.
Gunner, M. R., & Honig, B. (1991) *Proc. Natl. Acad. Sci. U.S.A. 88*, 9151–9155.
Hacker, B., Barquera, B., Crofts, A. R., & Gennis, R. B. (1993) *Biochemistry 32*, 4403–4410.
Hauska, G., Herold, E., Huber, C., Nitschke, W., & Sofrova, D. (1989) *Z. Naturforsch., C: Biosci. 44*, 462.
Howell, N. (1989) *J. Mol. Evol. 29*, 157–169.
Howell, N. (1990) *Biochemistry 29*, 8970–8977.
Howell, N., & Nalty, M. (1987) *Somatic Cell Mol. Genet. 13*, 529–537.
Howell, N., & Gilbert, K. (1988) *J. Mol. Biol. 203*, 607–618.
Kamensky, Y., Konstantinov, A. A., Kunz, W., & Surkov, S. (1985) *FEBS Lett. 181*, 95–99.
Kassner, R. J. (1972) *Proc. Natl. Acad. Sci. U.S.A. 69*, 2263–2267.
Konstantinov, A. A. (1990) *Biochim. Biophys. Acta 1057*, 138–141.
Konstantinov, A. A., & Popova, E. (1987) in *Cytochrome Systems: Molecular Biology and Bioenergetics* (Papa, S., Chance, B., Ernster, L., & Jaz, J., Eds.) pp 751–765, Plenum Press, New York.
Kunz, W. S., & Konstantinov, A. A. (1983) *FEBS Lett. 155*, 237–240.
Lee, K.-B., Jun, E., La Mar, G. N., Rezzano, I. N., Pandey, R. K., Smith, K. M., Walker, F. A., & Buttlaire, D. H. (1991) *J. Am. Chem. Soc. 113*, 3576–3583.
Link, T. A., & von Jagow, G. (1986) *FEBS Lett. 204*, 9–15.
Ljungdahl, P. O., Pennoyer, J. D., & Trumpower, B. L. (1986) *Methods Enzymol. 126*, 181–191.
Lubben, M., Kolmerer, B., & Saraste, M. (1992) *EMBO J. 11*, 805–812.
Makinen, M., & Churg, A. K. (1983) in *Iron Porphyrins, Part I* (Lever, A. B. P., & Gray, H. B., Eds.) pp 141–235, Addison-Wesley, Reading, MA.
Mandal, A. B., & Nair, B. U. (1991) *J. Phys. Chem. 95*, 9008–9013.
Matsuura, K., Bowyer, J. R., Ohnishi, T., & Dutton, P. L. (1983) *J. Biol. Chem. 258*, 1571–1579.
Meinhardt, S. W., & Crofts, A. R. (1982) *FEBS Lett. 149*, 217–222.
Mitchell, P. (1976) *J. Theor. Biol. 62*, 327–367.
Moore, G. R. (1983) *FEBS Lett. 161*, 171–175.
Moore, G. R., & Pettigrew, G. W. (1990) in *Cytochromes c. Evolutionary, Structural and Physicochemical Aspects*, Springer-Verlag, Berlin.
Moser, C. C., Keske, J. M., Warncke, K., Farid, R. S., & Dutton, P. L. (1992) *Nature 355*, 796–802.
Ohnishi, T., Schagger, H., Meinhardt, S. W., LoBrutto, R., Link, T. A., & von Jagow, G. (1989) *J. Biol. Chem. 264*, 735–744.
Rich, P. R. (1984) *Biochim. Biophys. Acta 768*, 53–79.
Rich, P. R., Jeal, A. E., Madgwick, S. A., & Moddy, A. J. (1990) *Biochim. Biophys. Acta 1018*, 29–40.
Robertson, D. E., & Dutton, P. L. (1988) *Biochim. Biophys. Acta 935*, 273–291.
Robertson, D. E., Daldal, F., & Dutton, P. L. (1990) *Biochemistry 29*, 11249–11260.
Robertson, D. E., Ding, H., Chelminski, P. R., Slaughter, C., Hsu, J., Moomaw, C., Tokito, M., Daldal, F., & Dutton, P. L. (1993) *Biochemistry 32*, 1310–1317.
Salerno, J. C. (1984) *J. Biol. Chem. 259*, 2331–2336.
Salerno, J. C., Xu, Y., Osgood, M. P., Kim, C. H., & King, T. E. (1989) *J. Biol. Chem. 264*, 15398–15403.
Schagger, H., Link, T. A., Engel, W. D., & von Jagow, G. (1986) *Methods Enzymol. 126*, 224–237.
Schmitt, M. E., & Trumpower, B. L. (1990) *J. Biol. Chem. 265*, 17005–17011.
Schomacker, K. T., & Champion, P. M. (1986) *J. Chem. Phys. 84*, 5314–5325.
Shelnutt, J. A. (1980) *J. Chem. Phys. 72*, 3948–3958.
Srajer, V., Schomacker, K. T., & Champion, P. M. (1986) *Phys. Rev. Lett. 57*, 1267–1270.
Stellwagen, E. (1978) *Nature 275*, 73–74.
Sutherland, J. C., & Klein, M. P. (1972) *J. Chem. Phys. 57*, 76–86.
Trumpower, B. L. (1990) *Microbiol. Rev. 54*, 101–129.
Tsai, A. H., & Palmer, G. (1982) *Biochim. Biophys. Acta 681*, 484–495.
Valentine, J. S., Sheridan, R. P., Allen, L. C., & Kahn, P. C. (1979) *Proc. Natl. Acad. Sci. U.S.A. 76*, 1009–1013.
Varadarajan, R., Lambright, D. G., & Boxer, S. G. (1989a) *Biochemistry 28*, 3771–3781.
Varadarajan, R., Zewert, T. E., Gray, H. B., & Boxer, S. G. (1989b) *Science 243*, 69–72.
von Jagow, G., & Ohnishi, T. (1985) *FEBS Letters 185*, 311–315.
von Jagow, G., & Link, T. A. (1986) *Methods Enzymol. 126*, 253–271.
West, I. C. (1989) *Biochim. Biophys. Acta 976*, 182–189.
West, I. C., Mitchell, P., & Rich, P. R. (1988) *Biochim. Biophys. Acta 933*, 35–41.
Widger, W. R., Cramer, W. A., Hermann, R. G., & Trebst, A. (1984) *Proc. Natl. Acad. Sci. U.S.A. 81*, 674–678.
Yun, C.-H., Crofts, A. R., & Gennis, R. B. (1991) *Biochemistry 30*, 6747–6754.
Yun, C.-H., Wang, Z., Crofts, A. R., & Gennis, R. B. (1992) *J. Biol. Chem. 267*, 5901–5909.